JOURNAL OF BIOMEDICAL OPTICS 1(4), 425–434 (OCTOBER 1996)

CHARACTERIZATION OF FEMALE BREASTS *IN VIVO* BY TIME RESOLVED AND SPECTROSCOPIC MEASUREMENTS IN NEAR INFRARED SPECTROSCOPY

Hans Heusmann, Jochen Kölzer, and Gerhard Mitic†
†Siemens AG, Corporate Research and Development, Otto-Hahn-Ring 6, D-81739 München, Germany

(Paper JBO/NIR-01 received Mar. 25, 1996; revised manuscript received July 15, 1996; accepted for publication July 22, 1996)

ABSTRACT

Time-resolved and spectroscopic *in vivo* measurements were performed to determine the optical properties of the female breast in transmission. The time-resolved measurements were carried out at different positions on the female breast with a Ti:sapphire laser (800 nm) using a synchroscan streak camera. A diffusion model was used to calculate the absorption coefficient μ_A and the reduced scattering coefficient. In addition, spectroscopic *in vivo* measurements of more than 100 patients were performed in a wavelength range between 650 and 1000 nm. A variety of pathological alterations could be characterized by measuring patients of different ages, different breast sizes, and at varying locations on the breast. The results indicate that besides the pure detection of the amount of blood in the neovascular network, the volume concentrations of water and fat seem to be of particular importance for discrimination. In order to quantify this observation, an analytical model was developed that takes the volume percentages of fat and water, the concentration and oxygenation of hemoglobin, and the relevant optical parameters into account. Experiments were carried out with volunteers and patients in a clinical environment: Typical observations are presented and analyzed statistically.

Keywords near infrared spectroscopy; time-resolved measurements; transillumination; breast cancer; optical tissue parameters.

1 INTRODUCTION

This review summarizes the results of previous papers concerning *in vivo* breast transillumination experiments.[1–5] In the first part, the time-resolved *in vivo* measurements for determining the optical properties of breast tissue are described.[1–3] In the second part, spectral *in vivo* measurements obtained by transilluminating the breasts of volunteers[4,5] and patients[5] in the diagnostic window (650 to 1000 nm) are presented. Important information about the wavelength-dependent transmission characteristics of benign and malignant lesions may be obtained in this way.

The determination of the absorption and scattering properties of tissue *in vivo* is of great interest for the noninvasive diagnosis of organs by light. Of particular interest in this area is the transillumination of the female breast for a preventive checkup.[6,7] Because of the potential hazards associated with x-ray exposure, harmless light-screening techniques may be an alternative to conventional x-ray mammography, or they may at least provide additional diagnostic information.

Many papers have been devoted to the determination of the optical properties of excised tissue specimens by means of extinction, absorption, and scattering angular distribution measurements.[8–11] Besides these steady-state methods, time-resolved reflectance and transmittance measurements have been used for the noninvasive determination of the optical properties of tissue.[12,13] The temporal spreading of a short light pulse in tissue due to multiple light scattering allows the optical coefficients to be determined [Figure 1(a)]. Because of the immense light scattering in tissue, most photons travel more than ten times the geometric distance between entering and leaving the tissue. The attenuation of multiple scattered photons thus allows the absorption and scattering properties of biological tissue to be determined quantitatively.

Very few *in vivo* data on the female breast[14,15] have hitherto been available. We therefore performed time-resolved *in vivo* experiments on volunteers using a Ti:sapphire laser at a wavelength of 800 nm. This wavelength is well suited for this purpose because it is the isosbestic point of oxy- and deoxyhemoglobin and the transmission is very high. The optical properties are determined by fit-

Address all correspondence to Hans Heusmann. E-mail: hans.heusmann@zfe.siemens.de

1083-3668/96/$6.00 © 1996 SPIE

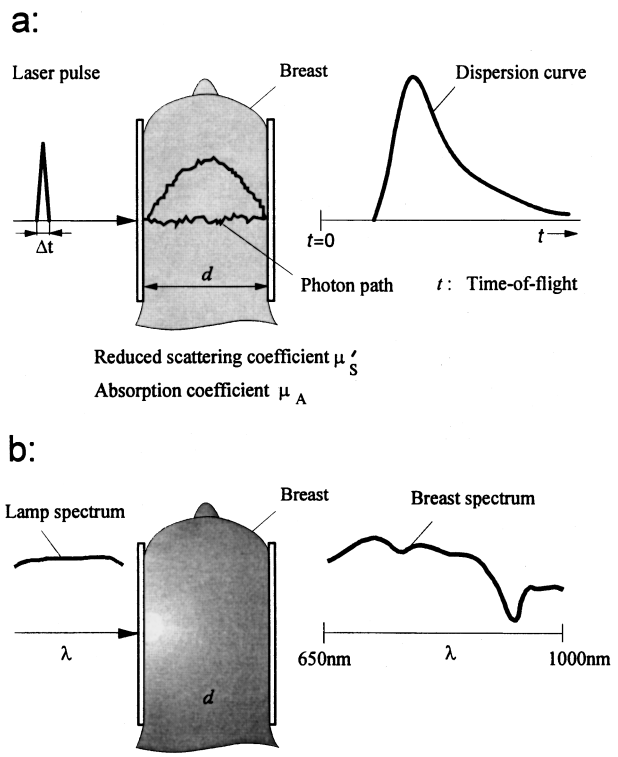

Fig. 1 Time-resolved (a) and spectroscopic (b) measurements on breast tissue *in vivo*.

ting the resulting dispersion curves to solutions of the diffusion model.[12]

Optical breast imaging, known as diaphanoscopy or diaphanography, is needed in clinical practice.[16–24] The question as to whether (pathologically) altered tissue differs from the surrounding (healthy) tissue, and whether criteria can also be found for differentiating between benign and malignant lesions is of central importance for approaches to imaging. A good contrast is produced when the optical parameters (absorption and scattering coefficients) of different types of tissue differ. It may also be due to physiological changes (tissue oxygen-saturation monitoring[25]). Some tissues exhibit a higher metabolic rate than others (many breast cancers, for example). In order to analyze the contributions from these physiological and morphological factors, optical spectroscopy is required [Figure 1(b)]. The goal is to optimize the contrast by selecting the appropriate wavelengths.[4,26,27] Practically all previous breast-imaging systems were equipped with measuring units for at least two wavelengths (diaphanography).[16–21] Prototype breast scanners[22,23] which combine time resolution and wavelength separation (an approach that has been developed for other applications[24,28]) are already undergoing clinical trials.

In this study, therefore, healthy and diseased breasts are characterized *in vivo* over the whole diagnostic window. An analytical model was developed to quantify the differences in the spectra. The

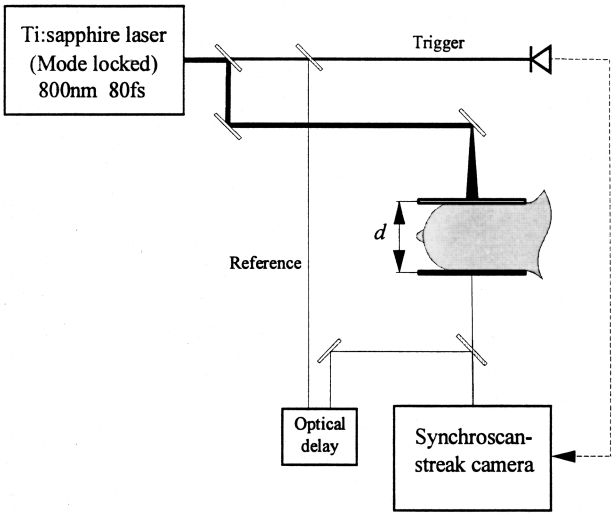

Fig. 2 Schematic setup for time-resolved transillumination of female breast tissue *in vivo*.

fitting parameters obtained are verified on the basis of ''medical plausibility factors'' and initial statistical correlations are attempted. This procedure is purely phenomenological and makes no claim to be exact. However, there is some hope that approaches to a specific diagnosis of breast carcinoma can be found by means of spectral light transillumination.

2 TIME-RESOLVED MEASUREMENTS

2.1 EXPERIMENTAL METHOD

The experimental setup for time-resolved light transillumination is shown schematically in Figure 2 (for details see Reference 3). The laser system for *in vivo* experiments consists of a mode-locked Ti: sapphire laser at a wavelength of 800 nm with a pulse width of 80 fs and a repetition frequency of 82 MHz.

Probe beam light is scattered in the female breast (which is slightly compressed between two transparent plates) and finally reaches the detection side of the synchroscan streak camera (S1 photocathode, Hamamatsu C3681) after many scattering events. This diffuse light is imaged onto the slit of the streak camera with a 1:1 magnification. The reference beam does not traverse the breast but is optically delayed and imaged on the streak camera slit to provide a temporal reference. The slit has dimensions of 50 μm$\times$6 mm and the numerical aperture of the camera optics is 0.22. A trigger beam synchronizes the streak camera. The temporal profile of the incident light intensity is recorded with a time resolution of about 10 ps and displayed as a spatial profile. To correct the measured dispersion curve, a precise shading correction and dark count subtraction were performed for each measurement.

2.2 DETERMINATION OF OPTICAL PARAMETERS

The optical properties of tissue can be deduced from the temporal dispersion curve. The diffusion model was used to determine the absorption coefficient μ_A and the reduced scattering coefficient $\mu_s' = \mu_s(1-g)$ (g is the anisotropy factor of scattering). A solution of the diffusion equation for a homogeneous medium of thickness d was applied according to Patterson et al.[12] The transmittance at a radial position ρ is given by

$$T(\rho,d,t) = \frac{1}{(4\pi Dc)^{3/2}t^{5/2}}\exp(-\mu_A ct) \times \exp\left(-\frac{\rho^2}{4Dct}\right)\left\{(d-z_0)\exp\left[-\frac{(d-z_0)^2}{4Dct}\right] - (d+z_0)\exp\left[-\frac{(d+z_0)^2}{4Dct}\right] + (3d-z_0)\exp\left[-\frac{(3d-z_0)^2}{4Dct}\right] - (3d+z_0)\exp\left[-\frac{(3d+z_0)^2}{4Dct}\right]\right\}. \quad (1)$$

The diffusion coefficient D is given by $D=[3(\mu_a+\mu_s')]^{-1}$, and $z_0=(\mu_s')^{-1}$ indicates the depth at which the incident photons are initially scattered. c stands for the speed of light within the breast.

It turned out that the diffusion model describes the light propagation in the breast fairly well as long as the reduced scattering length (reciprocal scattering coefficient) is smaller than 1/20 of the specimen thickness (i.e., as long as the angular distribution of the scattered light is isotropic). Both the reduced scattering coefficient μ_s' and the absorption coefficient μ_A can be determined by fitting the measured curve with the calculated temporal dispersion curve.[13]

2.3 *IN VIVO* EXPERIMENTS

For the *in vivo* measurements, the probe beam with a total power of 100 to 150 mW was expanded to a diameter of 10 mm to keep the power density below the maximum permissible exposure (MPE)[29] of 2 mW/mm^2, which corresponds to the solar constant. This power density does not cause perceptible heating of the illuminated skin. A beam blocker allowed the volunteers to interrupt the probe beam during the measurements. The breast was compressed to ensure a constant thickness, but much less than in conventional mammography to avoid any influence of changed blood perfusion on the absorption properties. Measurements were carried out with volunteers aged between 25 and 43 years.

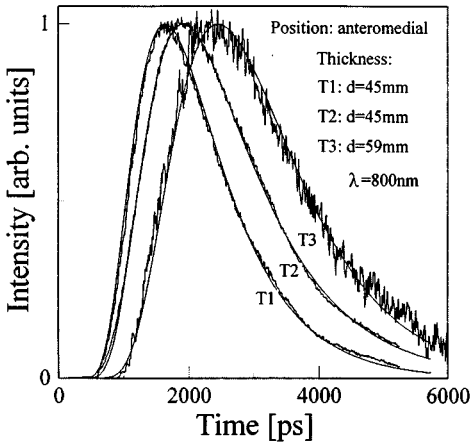

Fig. 3 Normalized *in vivo* dispersion curves of the breasts of three volunteers—T1, T2, and T3—(thickness d) and corresponding theoretical fit curves.

Normalized dispersion curves for three volunteers T1, T2, and T3 and the corresponding theoretical curves which were calculated according to the diffusion model [Eq. (1)] are shown in Figure 3. For the mathematical fit, we assumed the refractive index of breast tissue to be 1.4.[30,31] The time origin is given by the incidence of the laser pulse into the breast. The dispersion curves range over a typical period of 6 ns with a mean time of flight of more than 2 ns. Accordingly, most photons travel ten times the geometrical distance through the breast due to the strong scattering and the relatively weak absorption of the tissue. The signals T1 and T2 ($d=45$ mm) overcome the background noise after a time of flight of 510 ps, which is more than twice the minimum time-of-flight of a ballistic photon (refractive index 1.4). For dispersion curve T3 ($d=59$ mm) this time shifts to 830 ps, which is about three times longer than the minimum time of flight. The lower signal-to-noise ratio of curve T3 is due to the greater thickness of the compressed breast compared with volunteers T1 and T2.

Measurements at different positions of the breast were performed to show the influence of physiological alterations (different types of tissue, different blood volumes and oxygenation). Figure 4 shows measurements at the lateral, anteromedial, and medial position of the breast of volunteer T3. The normalized temporal dispersion curves of the lateral and medial positions agree well, whereas the curve of the anteromedial position is shifted to shorter times and shows a slower exponential decay. It is open to question whether this observation could be due to the slightly different boundary conditions of the anteromedial position. An identical breast thickness (59 mm) was chosen at the three measurement positions, but the enhanced anteromedial position near the nipple of the breast could reduce the mean time of flight.

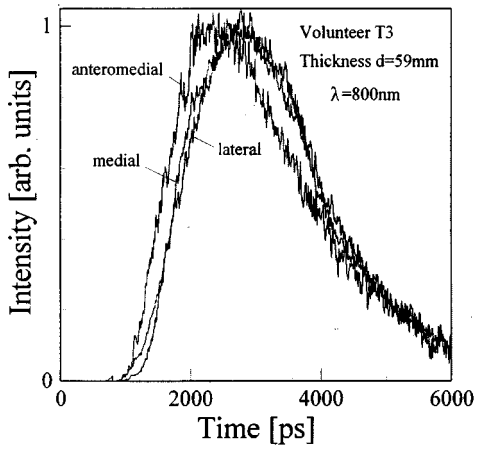

Fig. 4 Normalized temporal dispersion curves of the breast *in vivo* at the lateral, anteromedial, and medial position (volunteer T3).

The corresponding optical parameters of the fit curves are summarized in Table 1. Because breast tissue is inhomogeneous, consisting of adipose, glandular, and fibrocystic types of tissue, only mean optical parameters of the breast are represented by these values. Reduced scattering coefficients for human breast tissue *in vivo* at a wavelength of 800 nm range from μ_s'=0.72 mm^{-1} to μ_s'=1.35 mm^{-1} and corresponding absorption coefficients from μ_A=0.0017 mm^{-1} to μ_A=0.0045 mm^{-1}. The anteromedial position shows a lower scattering and absorption coefficient than the lateral and medial positions. This could be consistent with the above-mentioned different boundary conditions of the anteromedial position as well as with the anatomy of the female breast: the lateral and medial positions have a higher content of adipose tissue, whereas glandular tissue dominates at the anteromedial position. Consistent with our previous *in vitro* results[1] and with the investigations of Key et al.,[8] we nevertheless assume that adipose tissue shows a greater reduced scattering coefficient than glandular tissue. This conclusion should be verified by statistically more significant measurements.

Table 1 Reduced scattering and absorption coefficients for breast tissue *in vivo* at 800 nm (compressed thickness *d*).

			Fit parameter 800 nm	
Volunteer	Age (yrs.)	Thickness *d* (mm)	μ_s' (mm^{-1})	μ_A (mm^{-1})
T1 (Figure 3)	39	45	1.09	0.0032
T2 (Figure 3)	34	45	1.22	0.0022
T3 (Figure 4):	43	59		
anteromedial			1.05	0.0031
lateral			1.35	0.0045
medial			1.33	0.0045
T4 (not shown)	26	49	1.10	0.0028
T5 (not shown)	42	59	0.72	0.0017
T6 (not shown)	27	49	1.00	0.0019

The geometric conditions of the *in vivo* experiments differ from the idealized condition of the diffusion model. This source of systematic errors has been minimized by positioning the probe beam in the middle of the breast near the chest wall. Moreover, the compression varies from case to case. However, the reproducibility of the maximum of the temporal dispersion curve was about 4% when the measurement was repeated at the same location after repositioning. Thus the reduced scattering coefficient μ_s' can be determined with a reproducibility of about $\pm 5\%$. Regarding the ''geometrical boundary conditions'' of the breast, the absorption coefficient mostly had too high values because of lost photons; this effect limits measurable absorption coefficients to $\mu_a' \geqslant 0.001$ mm^{-1}.

It is impossible to determine the scattering coefficient μ_s and the anisotropy factor g independently of each other with the present experimental setup. As a consequence, the optical parameters were fitted only with respect to the reduced scattering coefficient $\mu_s' = \mu_s(1-g)$ and the absorption coefficient μ_A for all experiments. Published g values for different types of human breast tissues vary strongly. Values given by Key et al.[8] ($\lambda = 700$ nm) range from $g = 0.92$ for fibroglandular tissue and 0.95 for adipose tissue to 0.88 for carcinomas, while Peters et al.[9] measured g for all types of tissue in the range of 0.945 to 0.985 and showed it to be invariant with wavelength. However, the use of these strongly varying g values is of limited value for a calculation of μ_s.

Cheong et al.[11] gave an overview of the optical properties of biological tissues. However, the literature offers few references to the optical parameters of human breast tissue *in vivo*[3,13–15] and these were determined only at fixed wavelengths. Some authors distinguish between different types of breast tissue *in vitro*[8,9] although these measurements are again limited to only a few wavelengths.

3 SPECTROSCOPIC MEASUREMENTS

3.1 EXPERIMENTAL

The spectral experiments were conducted using a commercially available spectroradiometer (Merlin from the Oriel Company) (Figure 5). The light source was a 100-W tungsten-halogen lamp with a uniformly high spectral radiation intensity inside the relevant measurement range of 550 and 1050 nm; a monochromator was fitted with a 600

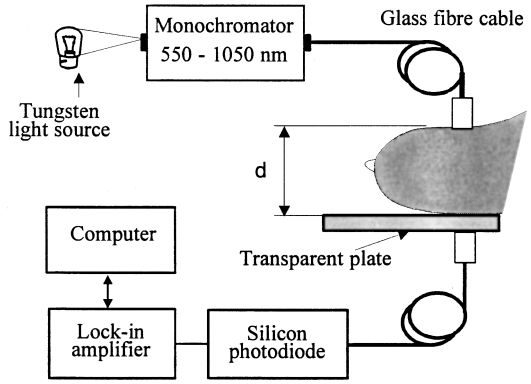

Fig. 5 Schematic setup of the spectroradiometer system used for *in vivo* measurements.

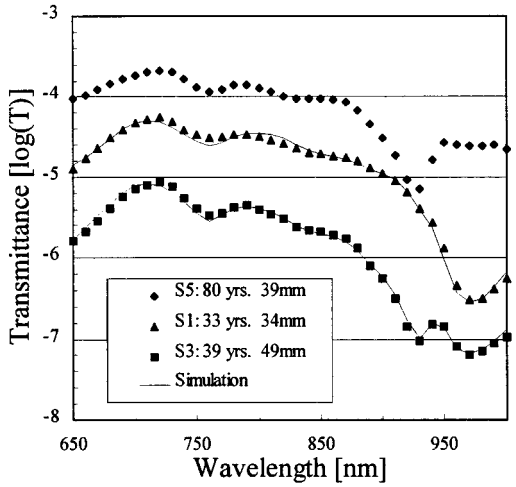

Fig. 6 *In vivo* spectra and the respective fits (see Table 3 for values) of three persons of different ages at the same measurement site.

lines/mm grating and a linear reciprocal dispersion of 12.8 nm/mm (at the blaze wavelength of 750 nm). All measurements were performed in transmission mode. The breast was placed onto a transparent plate and the illuminated optical fiber head (5 mm diameter) was placed directly onto the skin under slight pressure. The light intensity of about 5 mW/cm^2 on the skin was far below the maximum permissible exposure.[29] The transmitted light was detected by a 2-m long optical fiber cable coupled to a silicon photodiode. The time required for a single measurement was approximately 150 s, 50 points being measured (in 10-nm steps). The recorded intensities were divided by the input intensities $I/I(0)$ and plotted as the decadic logarithm of the transmittance. This enables the spectral profile of the instrument to be taken into account and provides a reliable measure of the total percentage attenuation (optical density). Each spectrum was measured at a fixed location, mostly at several positions on the same breast. Transmission spectra from breasts measured *in vivo* vary by two to three orders of magnitude for each curve, and the curves cover an overall range of almost seven decades for the investigated thicknesses from 26 to 80 mm[5] (Figure 6; three selected spectra can be seen). However, each curve showed similar spectral characteristics: (1) a decrease in transmittance by several orders of magnitude below 600 nm (blood absorption), (2) transmission minima at about 760 nm (superposition of Hb and weaker water and fat signals), and (3) more or less pronounced minima at 930 nm (fat) and 975 nm (water) with different peak relationships that contain specific information about the tissue composition (see Sec. 3.3).

3.2 ANALYTICAL MODELING

An attempt was made[5] to obtain an analytical fit of the *in vivo* breast spectra by making use of highly simplifying assumptions: First, the breast tissue is regarded as a homogeneous mixture of four absorbing media, namely, water, fat, deoxyhemoglobin, and oxyhemoglobin. Second, the constituents of water and fat together amount to 100% by volume. Third, the volumetric constituents of Hb and HbO_2 are neglected (only 2.3 mmol per liter of blood). Finally, the absolute values and the wavelength dependence of the required absorption coefficients of these constituents were obtained from the literature[32] or were measured by the authors (Figure 7). The reduced scattering coefficients of the breast tissue *in vivo* were obtained by extrapolating the results of our time-resolved measurements *in vivo* and *in vitro* (Figure 8).

In an exclusively absorbing medium with an absorption coefficient μ_a and thickness d, the attenuation of a beam of light having an initial intensity I_0 can be described by the Beer-Lambert law:

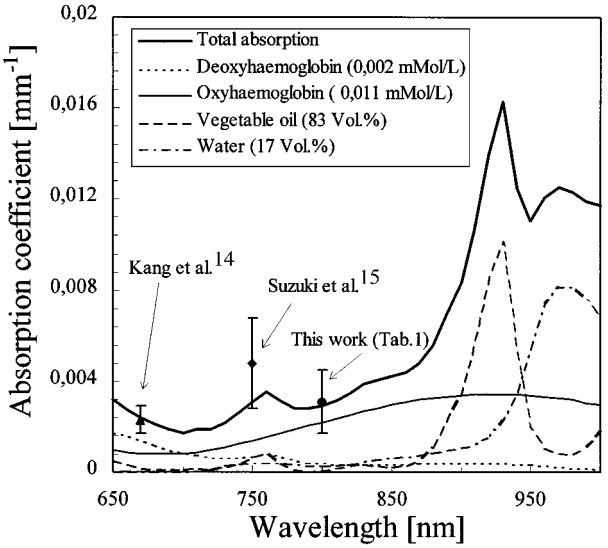

Fig. 7 Absorption coefficients of deoxy- and oxyhemoglobin,[32] water, and fat (vegetable oil).

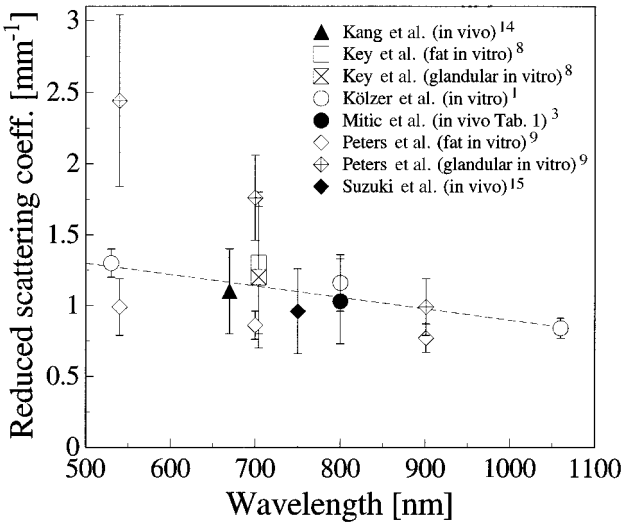

Fig. 8 Reduced scattering coefficients for human breast tissue *in vivo* and *in vitro* measured at different wavelengths. By extrapolating *in vitro* values (Kölzer et al.[1]), scattering coefficients over the whole spectral range are approximated (dotted line).

$$I = I_0 \times \exp(-\mu_a \times d). \tag{2}$$

The total absorption μ_a can then be calculated as a sum of the specific absorption coefficients α_i (absorber i) multiplied by their respective concentrations c_i:

$$\mu_a = c_{\text{water}}\alpha_{\text{water}} + c_{\text{fat}}\alpha_{\text{fat}} + c_{\text{Hb}}\alpha_{\text{Hb}} + c_{\text{HbO}}\alpha_{\text{HbO}}. \tag{3}$$

However, this simple law will no longer apply if multiple scattering also occurs, because the path of the individual photons is unknown. Patterson et al.[12] have shown that with the assumption of a plane-parallel geometry, the diffusion equation can be used to calculate a mean path length L of the photons:

$$L = \left[\frac{4\mu_a}{3(\mu_a + \mu_s')}\right]^{-1/2} \times \frac{\left(d - \frac{1}{\mu_s'}\right)\exp\left\{\frac{2}{\mu_s'}\left[\mu_a 3(\mu_a + \mu_s')\right]^{1/2}\right\} - \left(d + \frac{1}{\mu_s'}\right)}{\exp\left\{\frac{2}{\mu_s'}\left[\mu_a 3(\mu_a + \mu_s')\right]^{1/2}\right\} - 1}. \tag{4}$$

In order to take the multiple scattering into account, we replaced the thickness d in the Beer-Lambert law [Eq. (2)], by the mean path length $L(\lambda)$. The transmitted intensity may then be represented by:

$$I(\lambda) = I_0(\lambda) x_1 \exp[-\mu_a(\lambda) L(\lambda) x_2]. \tag{5}$$

To fit the absolute values of the transmittance for all spectra, another two wavelength-independent correction factors were introduced: x_1 takes into account multiply scattered but not absorbed photons, which do not arrive at the detector and the measurement geometry, while x_2 compensates for measurement errors of the thickness d and inaccuracies in the reduced scattering coefficient. By varying the concentrations of the four tissue components, the measurement spectra could be fitted well by the semiempirical formula (5). The correlation coefficients were better than 0.99 in all cases.

3.3 WAVELENGTH DEPENDENCY OF OPTICAL PARAMETERS OF BREAST TISSUE

The prime absorbers, namely blood, water, and fat, determine a diagnostic window for thick biological tissue *in vivo*: the limit for shorter wavelengths is approximately 600 nm (blood); that for longer wavelengths is approximately 1.4 μm (water). Because of our detector system (Si photodiode), the measurement range in the long-wavelength region is further limited to about 1.1 μm. Figure 7 shows the specific absorption coefficients of the two blood pigments deoxy- and oxyhemoglobin (Hb and HbO) between 650 and 1000 nm, as taken from the literature.[33] Within this wavelength range, the absorption maximum of Hb (760 nm) is significant. The features of Hb and HbO below these wavelengths (not shown, cf. Horecker[32]) are not relevant for *in vivo* applications to thick tissues. At the isosbestic point (805 nm), the absorption coefficients of Hb and HbO are equal. In addition, we calculated the corresponding absorption coefficients from the measured transmission characteristics of water and fat (vegetable oil). The main absorption feature of water is the O—H resonance at 975 nm. Weaker overtones of this resonance can be observed at 840 and at about 755 nm. The signal of fat (or the oil signal shown here) differs from water primarily in the infrared region. The main C—H resonance is located at 930 nm, while some weaker signals can be observed at 760 and 830 nm.[34] Thus the absorption coefficients in particular provide only a global reference point for the total absorption of the heterogeneous tissue body and are therefore not useful for the model described above.

The reduced scattering coefficients used are based on our *in vivo* and *in vitro* measurements,[1,3] and on *in vivo* data published by other authors,[14,15] Figure 8. However, these data do not allow us to distinguish meaningfully between different types of tissue (water- or fat-containing tissues). The (weak) wavelength dependence of the reduced scattering coefficients shown in Figure 8 describes reality in qualitative terms, and suffices for our purposes.

3.4 SPECTRA OF FEMALE BREASTS *IN VIVO*

The aim of these measurements was to gain comprehensive spectral information on the absorption characteristics of the female breast *in vivo*. About 100 volunteers of different ages were examined in a

Table 2 Fit parameters of the *in vivo* spectra of younger and older persons (see Figure 6).

		Fit parameter		
Volunteer	Age (yrs.)	Water (vol.%)	Hb (mMol/L)	HbO (mMol/L)
S1	33	70	0,0020	0,0041
S2	37	65	0,0017	0.0042
S3	39	33	0,0012	0,0042
S4	64	12	0,0005	0,0018
S5	80	11	0,0002	0,0014
S6	85	17	0,0005	0,0030

clinical environment. The investigation concentrated on taking measurements at various sites on the same breast as well as on comparative readings at equivalent sites on both breasts. Differences in tissue composition (age, measurement points, etc.) result in a change of the absorption and scattering coefficients and consequently in a modified spectrum. The analytical model described in Sec. 3.2, which yields the concentrations of water, fat, Hb and HbO as fit parameters, is needed to quantify these changes.

3.4.1 Physiological Alterations

The changes occurring in the female breast with increasing age are characterized by an involution of the glandular body and an expansion of the fatty tissue. The water and hemoglobin concentrations calculated from the spectra using our model match this physiological fact. Table 2 shows the fit parameter of the spectra of six volunteers at the same measurement site but of different ages. The respective fits of three transmission spectra are shown in Figure 6. High water and hemoglobin concentrations are typical of the younger volunteers (S1, S2, S3), whose breasts have a glandular body that is bigger, contains more water, and is better perfused with blood. Higher fat content is correlated with a lower metabolic rate and hence with a lower oxygen consumption. The older women (S4, S5, S6) with breasts consisting mostly of fatty tissue consequently show lower water and blood contents and a higher tissue oxygenation (HbO/(HbO+Hb)).[5] The water content of breasts of younger and older persons determined according to our model is directly compared in Figure 9. Each of the two groups of patients examined consisted of more than 20 persons. Those in the first group were aged between 30 and 45 years, and those in the second between 55 and 80 years. The water content of the breast tissue varied between 5 and 75%, its relative distribution being determined in steps of 10% (5 to 15%, 16 to

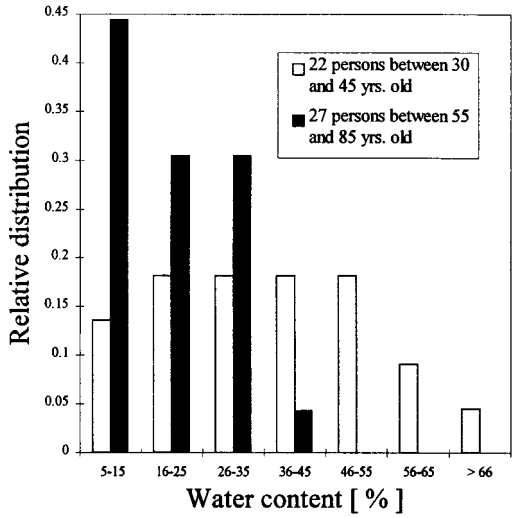

Fig. 9 Frequency distribution of water concentration for older and younger women.

25%, etc.). The distribution shows significant differences in the two age groups. A relatively low water content (<35%) was seen with significantly higher frequency in older breast tissue than in younger tissue. The highest value that we found in the former was below 45%, whereas the latter reached a water content of 75%. The water-content distribution function for younger breast tissue is generally flat and covers the entire range between 5 and 75%.

In order to characterize local variations in water, fat, oxy- and deoxyhemoglobin concentrations, the spectra of eight volunteers were recorded at three different sites on a woman's breast. The spectra of the lateral, anteromedial, and medial sites were fitted as described above (Figure 10; only two curves are shown), while the fit parameters (concentration of water and hemoglobin) are shown in Figures 11 and 12. The increase in the water and hemoglobin

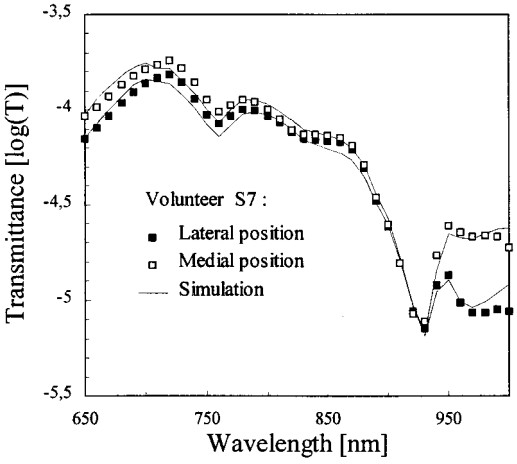

Fig. 10 Two selected *in vivo* spectra of the female breast at different sites from the same volunteer. The spectra of all three sites were fitted analytically (Table 2).

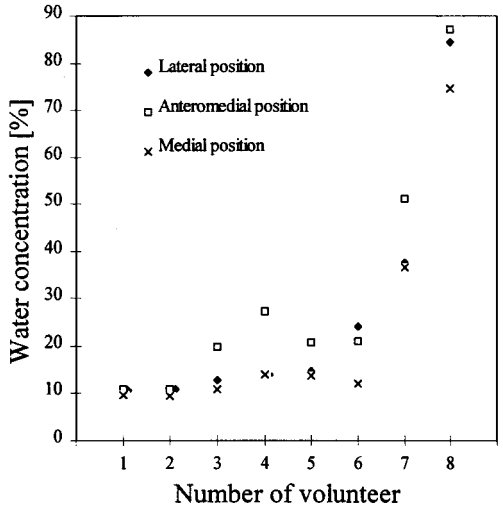

Fig. 11 Water concentration of eight volunteers at three different measurement sites on the breast. The anteromedial and the lateral position, where the glandular body is located, show a higher water content than the medial position.

concentration toward the anteromedial and lateral side has a plausible physiological explanation. The glandular body, which is situated at the lateral side of the breast and extends to the nipple, has a higher water content and blood perfusion than the surrounding fatty tissue. The medial side of the breast has a higher fat content, which seems to be correlated with a higher blood oxygenation (fit parameter not shown).

3.4.2 Malignant and Benign Breast Lesions

In the clinical part of our project, *in vivo* spectra were measured for several persons suffering from breast cancer and benign breast lesions (mainly

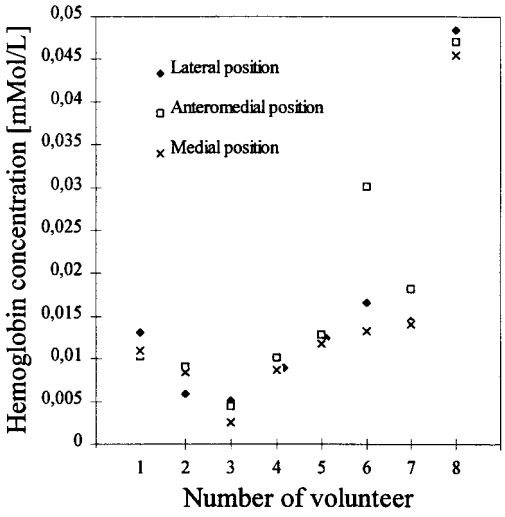

Fig. 12 Blood concentration (sum of oxy- and deoxyhemoglobin) of eight volunteers at three different measurement sites on the breast. The medial position shows in most cases a lower blood concentration.

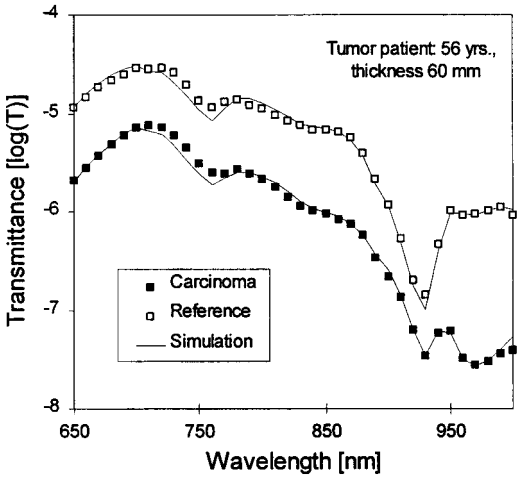

Fig. 13 *In vivo* spectra and respective fits of a breast cancer patient. The reference spectrum represents a measurement at the mirror position of the healthy breast.

mastopathies). A prior diagnostic finding (from palpation, mammography, breast ultrasonography or magnetic resonance imaging) was available in all cases, allowing the lesion to be localized and transilluminated at a fixed site with a high degree of accuracy. Patients were subjected to two measurements: one of the pathological breast and at least one control measurement at an equivalent point on the healthy breast. The breast tissue of patients undergoing biopsy and mastectomy was subjected to histological classification. This procedure allowed the selection of *in vivo* spectra that had been measured preoperatively in a cancerous breast. A measurement was always also performed at the mirror position in the healthy breast, which was compressed to the same thickness. This mirror spectrum was used as a direct reference for the spectrum of the carcinoma.

The following observations were typical (Figure 13): first, most carcinoma curves exhibit a lower transmittance than the reference curve (for the same breast thickness). The fits show in an exemplary way that this is generally due to an increased perfusion (higher Hb/HbO values of the carcinoma curve). Second, the different curve profile in the wavelength region between about 900 and 1000 nm is striking. This is clearly due to an altered water and fat content compared with that of the healthy breast. In Figure 14 we summarize these results by splotting the difference in water concentration between the healthy and diseased breast versus the respective difference in blood volume. Each pixel represents an individual patient. If a higher water and blood content (sum of Hb and HbO concentration) is present at the lesion site, a measuring symbol will appear in the lower right quadrant. Mastopathies are represented by crosses, carcinomas by filled squares. The majority of mastopathies and carcinomas show a higher water concentration and

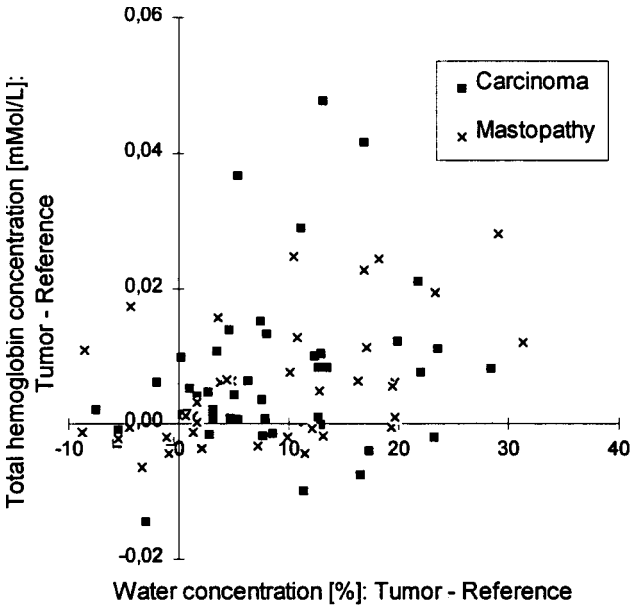

Fig. 14 Difference in water concentration between diseased and healthy breast versus respective difference in blood volume. Most carcinomas and mastopathies show higher water and blood content (upper right quadrant).

a higher blood volume at the lesion site (upper right quadrant). Only very few lesions have a lower water and blood concentration (lower left quadrant). Additional information could be obtained by calculating the degree of blood oxygenation from the concentrations of oxy- and deoxyhemoglobin.

A comparison of healthy and cancerous sites yields a slightly lower degree of oxygenation for the tumor. Note that the fit parameters are based on the very simplified assumption of our semiempirical model as mentioned in Sec. 3.2. This means that the local change of water and blood concentration at the lesion is underestimated by our assumption of a homogeneous mixture of constituents, which leads to an integral volume sampling procedure. Considering this restriction, it is astonishing that a high sensitivity in the detection of lesions by measuring water concentration, blood volume, and blood oxygenation seems to be within reach. Unfortunately, however, the specificity is worse because it is not possible to discriminate between benign mastopathies and malignant carcinomas by means of water content, blood volume, and oxygenation.

4 SUMMARY

The optical parameters of the female breast were determined by time-resolved *in vivo* experiments at a wavelength of $\lambda = 800$ nm. In brief, the reduced scattering coefficients range from $\mu_s' = 0.72$ mm^{-1} to $\mu_s' = 1.35$ mm^{-1} and the corresponding absorption coefficients from $\mu_A = 0.0017$ mm^{-1} to $\mu_A = 0.0045$ mm^{-1}. The absorption coefficient of breast tissue is nearly three orders of magnitude smaller than the corresponding reduced scattering coefficient. Similar results have also been found by Kang et al. from measurements of the time-resolved reflectance of breast tissue *in vivo*.[14] The advantage of time-resolved measurements is that they allow direct detection of the extremely weak absorption of highly scattering media. The procedure is sensitive enough to detect variations in tissue composition, as demonstrated by measurements on different positions of the breast.

Furthermore, female breasts were characterized by spectroscopic measurements in the wavelength range between 650 and 1000 nm. All the experimental spectra can be sufficiently fitted by an analytical model. Physiological, age-related tissue changes in the breast and local variations in composition can be verified quantitatively. Moreover, a changed metabolic rate (higher perfusion, reduced oxygenation) can also be identified. Lesions in the breast can be detected by identifying the relative water (and fat), Hb, and HbO contents of the pathological tissue. Since benign lesions (mastopathies) show spectroscopic features similar to carcinomas, it will be difficult to discriminate between them. However, the implementation of ''specific'' wavelengths such as 930 and 980 nm in NIR imaging systems would improve the sensitivity and probably also the specificity of this technique. It is currently still uncertain whether this suggestion would enable a distinction to be made between malignant and benign lesions.

Acknowledgments

We would like to thank P. Krämmer, J. Otto, G. Sölkner, and W. Zinth for fruitful discussions. Special thanks are due to M. Guntersdorfer and E. Wolfgang for their general encouragement. The measurements were performed at the Universities of Leipzig and Halle. We particularly thank the physicians S. Heywang-Köbrunner, L. Götz, R. Puls, and H. Waak for their help.

REFERENCES

1. J. Kölzer, G. Mitic, J. Otto, and W. Zinth, ''Measurement of the optical properties of breast tissue using time-resolved transillumination,'' *Proc. SPIE* **2326**, 143–152 (1995).
2. G. Mitic, J. Kölzer, J. Otto, E. Plies, G. Sölkner, and W. Zinth, ''Time-resolved transillumination of turbid media,'' *Proc. SPIE* **2082**, 26–32 (1994).
3. G. Mitic, J. Kölzer, J. Otto, E. Plies, G. Sölkner, and W. Zinth, ''Time-gated transillumination of biological tissues and tissue-like phantoms,'' *Appl. Opt.* **33**, 6699–6710 (1994).
4. H. Heusmann, J. Kölzer, J. Otto, R. Puls, T. Friedrich, S. Heywang-Köbrunner, and W. Zinth, ''Spectral transillumination of female breasts and breast tissue-like material,'' *Proc. SPIE* **2326**, 370–382 (1995).
5. H. Heusmann, J. Kölzer, R. Puls, J. Otto, S. Heywang-Köbrunner, and W. Zinth, ''Spectral transillumination of human breast tissue,'' *Proc. SPIE* **2389**, 798–808 (1995).
6. O. Jarlman, G. Balldin, I. Andersson, M. Löfgren, A. S. Larsson, and F. Linell, ''Relation between light scanning and the histologic and mammographic appearance of malignant breast tumors,'' *Acta Radiologica* **33**, 63–68 (1992).
7. O. Jarlman, I. Andersson, G. Balldin, and S. A. Larsson, ''Diagnostic accuracy of light scanning and mammography in

women with dense breasts,'' *Acta Radiologica* **33**, 69–71 (1992).
8. H. Key, E. R. Davies, P. C. Jackson, and P. N. T. Wells, ''Optical attenuation characteristics of breast tissues at visible and near-infrared wavelengths,'' *Phys. Med. Biol.* **36**, 579–590 (1991).
9. V. G. Peters, D. R. Wyman, M. S. Patterson, and G. L. Frank, ''Optical properties of normal and diseased human breast tissues in the visible and near infrared,'' *Phys. Med. Biol.* **35**, 1317–1334 (1990).
10. R. Marchesini, A. Bertoni, S. Andreola, E. Melloni, and A. E. Sichirollo, ''Extinction and absorption coefficients and scattering phase functions of human tissues in vitro,'' *Appl. Opt.* **28**, 2318–2324 (1989).
11. W. F. Cheong, S. A. Prahl, and A. J. Welch, ''A review of the optical properties of biological tissues,'' *J. Quant. Electr.* **26**, 2166–2184 (1990).
12. M. S. Patterson, B. Chance, and B. C. Wilson, ''Time-resolved reflectance and transmittance for the noninvasive measurements of optical properties,'' *Appl. Opt.* **28**, 2331–2336 (1989).
13. R. Berg, S. Andersson-Engels, O. Jarlman, and S. Svanberg, ''Time-resolved transillumination for medical diagnostics,'' *Proc. SPIE* **1431**, 110–119 (1991).
14. K. A. Kang, B. Chance, S. Zhao, S. Srinivasan, E. Patterson, and R. Troupin, ''Breast tumor characterization using near-infrared spectroscopy,'' *Proc. SPIE* **1888**, 487–499 (1993).
15. K. Suzuki, Y. Yamashita, K. Ohta, and B. Chance, ''Quantitative measurement of optical parameters in the breast using time-resolved spectroscopy,'' *Invest. Radiol.* **29**, 410–414 (1994).
16. G. A. Navarro and A. E. Profio, ''Contrast in diaphanography of the breast,'' *Med. Phys.* **15**, 181–187 (1988).
17. E. Carlsen, ''Transillumination light scanning,'' *Diagnostic Imaging* **3**, 28–33, 60 (1982).
18. H. Key, P. C. Jackson, and P. N. T. Wells, ''New approaches to transillumination imaging,'' *J. Biomed. Eng.* **10**, 113–118 (1988).
19. H. Wallberg, A. Alveryd, and K. Carlsson, ''Breast carcinoma and benign breast lesions: Diaphanography and quantitative evaluation using the computer controlled image scanner OSIRIS,'' *Acta Radiologica Diagnosis* **26**, 535–541 (1985).
20. P. He, M. Kaneko, M. Takai, K. Baba, Y. Yamashita, and K. Ohta, ''Breast cancer diagnosis by laser transmission photoscanning with spectro-analysis (Report 4),'' *Radiation Med.* **8**, 1–5 (1990).
21. A. W. Domanski, ''Multilaser head for optoelectronic mammoscope,'' in *Lasers in Medicine*, W. Waidelich, R. Waidelich, and A. Hofstetter, Eds., pp. 489–492, Springer-Verlag, Berlin (1994).
22. M. Kaschke, H. Jess, G. Gaida, J. Kaltenbach, and W. Wrobel, ''Transillumination imaging of tissue by phase modulation techniques,'' in *Advances in Optical Imaging and Photon Migration*, R. R. Alfano, Ed., *OSA Proc.* **21**, 88–92 (1994).
23. A. Oppelt, O. Schütz, and H. Siebold, ''First clinical images of a 4-wavelength breast scanner,'' (Abst.), in *Integration of Medical Optical Imaging and Spectroscopy (MOI/MOIS) and Magnetic Resonance Imaging (MRI)*, University of Pennsylvania, Medical Center (1994).
24. A. Duncan, T. L. Whitlock, M. Cope, and D. T. Delpy, ''A multiwave, wideband, intensity modulated optical spectrometer for near infrared spectroscopy and imaging,'' *Proc. SPIE* **1888**, 248–257 (1993).
25. F. F. Jöbsis, ''Non-invasive infra-red monitoring of cerebral and myocardial oxygen sufficiency and circulatory parameters,'' *Science* **198**, 1264–1266 (1977).
26. S. Ertefai and A. E. Profio, ''Spectral transmittance and contrast in breast diaphanography,'' *Med. Phys.* **12**, 393–400 (1985).
27. R. L. Egan and P. D. Dolan, ''Optical spectroscopy: Premammography marker,'' *Acta Radiologica* **29**, 497–503 (1988).
28. S. Andersson-Engels, R. Berg, A. Persson, and S. Svanberg, ''Multispectral tissue characterization with time-resolved detection of diffusely scattered white light,'' *Opt. Lett.* **18**, 1697–1699 (1993).
29. IEC 825, ''Radiation safety of laser products, equipment classification, requirements and user's guide,'' International Electrotechnical Commission (1984) (modified 1990).
30. F. P. Bolin, L. E. Preuss, R. C. Taylor, and R. J. Ference, ''Refractive index of some mammalian tissues using a fiber optic cladding method,'' *Appl. Opt.* **28**, 2297–2303 (1989).
31. D. T. Delpy, M. Cope, P. van der Zee, S. Arridge, S. Wray, and J. Wyatt, ''Estimation of optical path length through tissue from direct time-of-flight measurement,'' *Phys. Med. Biol.* **33**(12), 1433–1442 (1988).
32. B. L. Horecker, ''The absorption spectra of hemoglobin and its derivatives in the visible and near infrared regions,'' *J. Biol. Chem.* **148**, 173–183 (1943).
33. M. Cope, ''The development of a near infrared spectroscopy system and its application for non invasive monitoring of cerebral blood and tissue oxygenation in the newborn infant,'' Thesis, University College London (1991).
34. K. H. Norris, ''Possible medical applications of NIR,'' in ''*Making Light Work: Advances in Near Infrared Spectroscopy*,'' I. Murray and I. A. Cowe, Eds., pp. 596–602, VCH-Verlag, Weinheim (1991).